Induction of oligoclonal CD8 T cell responses against pulmonary metastatic cancer by a phospholipid-conjugated TLR7 agonist

Tadashi Hosoya[a,b], Fumi Sato-Kaneko[a], Alast Ahmadi[a], Shiyin Yao[a], Fitzgerald Lao[a], Kazutaka Kitaura[c], Takaji Matsutani[c], Dennis A. Carson[a,1], and Tomoko Hayashi[a,1]

[a]Moores Cancer Center, University of California, San Diego, La Jolla, CA 92093-0695; [b]Graduate School of Tokyo Medical and Dental University, 113-8519, Tokyo, Japan; and [c]Repertoire Genesis Inc., Ibaraki-shi, 567-0085 Osaka, Japan

Contributed by Dennis A. Carson, June 4, 2018 (sent for review February 23, 2018; reviewed by Edgar G. Engleman and Stephen P. Schoenberger)

Recent advances in cancer immunotherapy have improved patient survival. However, only a minority of patients with pulmonary metastatic disease respond to treatment with checkpoint inhibitors. As an alternate approach, we have tested the ability of systemically administered 1V270, a toll-like receptor 7 (TLR7) agonist conjugated to a phospholipid, to inhibit lung metastases in two variant murine 4T1 breast cancer models, as well as in B16 melanoma, and Lewis lung carcinoma models. In the 4T1 breast cancer models, 1V270 therapy inhibited lung metastases if given up to a week after primary tumor initiation. The treatment protocol was facilitated by the minimal toxic effects exerted by the phospholipid TLR7 agonist compared with the unconjugated agonist. 1V270 exhibited a wide therapeutic window and minimal off-target receptor binding. The 1V270 therapy inhibited colonization by tumor cells in the lungs in an NK cell dependent manner. Additional experiments revealed that single administration of 1V270 led to tumor-specific $CD8^+$ cell-dependent adaptive immune responses that suppressed late-stage metastatic tumor growth in the lungs. T cell receptor (TCR) repertoire analyses showed that 1V270 therapy induced oligoclonal T cells in the lungs and mediastinal lymph nodes. Different animals displayed commonly shared TCR clones following 1V270 therapy. Intranasal administration of 1V270 also suppressed lung metastasis and induced tumor-specific adaptive immune responses. These results indicate that systemic 1V270 therapy can induce tumor-specific cytotoxic T cell responses to pulmonary metastatic cancers and that TCR repertoire analyses can be used to monitor, and to predict, the response to therapy.

lung metastasis | toll like receptor 7 agonist | T cell receptor repertoire analysis | cancer immunotherapy

Recent advances in cancer treatment have improved the survival and quality of life for patients, especially those who are in the early clinical stages (1). However, prolonged survival is still unachievable in most patients with advanced cancer that have distal metastases. In particular, metastases of primary tumors contribute to 90% of patient deaths (2). The lungs are the second most frequent site of metastases from extrathoracic malignancies (3). Cancer in the lungs can create an immunosuppressive and angiogenic microenvironment (4, 5). Recent studies suggest that immunotherapy with checkpoint inhibitors can overcome the immunosuppressive networks to prevent and, in some cases, to eradicate lung metastases (6, 7). However, checkpoint inhibitors achieve a progression-free survival in only 10–30% of patients with metastases (8, 9). Hence, there are strong demands for new immunotherapeutic approaches to improve survival rates of metastatic cancer patients.

A synthetic TLR7 agonist, imiquimod, has already been approved for human use and shows favorable clinical efficacy in patients with dermatological tumors, including basal cell carcinoma and actinic keratosis (10). However, the drug's applications are limited to topical use because of immunotoxicity induced by systemic administration (11, 12). To improve the pharmacokinetics and reduce severe immune adverse effects, our laboratory developed 1V270, a small molecule TLR7-specific ligand (1V136, SM360320) conjugated to a phospholipid moiety (13, 14). We demonstrated that intratumoral administration of 1V270 induces tumor-specific adaptive immune responses and inhibits primary tumor growth in murine syngeneic models of head and neck cancer and melanoma (15, 16). The local 1V270 treatment activates tumor-associated macrophages and converts an immune-suppressive tumor microenvironment to a tumoricidal environment without causing systemic cytokine induction (16). Subsequently, 1V270 therapy induced tumor-specific adaptive immune responses that suppressed tumor growth in uninjected tumors. Reports by others have demonstrated that the use of local or systemic TLR7 agonists, alone or as vaccine adjuvants, can induce tumor-specific immune responses and reduce the growth of colon, renal, and mammary carcinomas (17, 18).

In contrast to the therapeutic advantages of using TLR7 agonists on the innate immune cells in the tumor microenvironment, some recent reports indicate that TLR7 signaling pathway may promote tumor growth in primary lung carcinoma (19, 20). This phenomenon is attributable to increased recruitment of

Significance

A major goal of cancer immunotherapy is the expansion and/or reactivation of cytotoxic $CD8^+$ T cell responses against malignant cells. We previously showed that the direct injection of toll-like receptor 7 (TLR7) agonists into primary tumors can induce tumor-specific oligoclonal T cell responses whose magnitude correlates with therapeutic efficacy. However, tumors are not always accessible to local therapy. Here, we demonstrate in murine lung metastasis models that single systemic administration of a phospholipid conjugated TLR7 agonist can also expand tumor-specific cytotoxic T cells that are shared by different animals. The expansion can be achieved without causing apparent toxicity. Similar technology combining immune repertoire analysis and immunomodulatory drugs can help to guide the development of optimal immunotherapeutic regimens in cancer patients.

Author contributions: T. Hosoya, D.A.C., and T. Hayashi designed research; T. Hosoya, F.S.-K., A.A., S.Y., F.L., K.K., T.M., and T. Hayashi performed research; T. Hosoya, F.S.-K., K.K., T.M., D.A.C., and T. Hayashi analyzed data; and T. Hosoya, F.S.-K., D.A.C., and T. Hayashi wrote the paper.

Reviewers: E.G.E., Stanford University School of Medicine; and S.P.S., La Jolla Institute for Allergy and Immunology.

Conflict of interest statement: K.K. and T.M. are employees of Repertoire Genesis Inc.

Data deposition: TCR sequencing data is available in ArrayExpress (accession no. E-MTAB-6016).

[1]To whom correspondence may be addressed. Email: dcarson@ucsd.edu or thayashi@ucsd.edu.

This article contains supporting information online at www.pnas.org/lookup/suppl/doi:10.1073/pnas.1803281115/-/DCSupplemental.

Published online July 2, 2018.

myeloid-derived suppressor cells (MDSCs) to the tumor following TLR7 therapy (20, 21). Thus, TLR7 therapy may function as a double-edged sword depending on the type of tumor, the levels of receptor expression, and infiltration of suppressor cells in the tumor microenvironment (22). In this study, we evaluated the effects of 1V270 therapy on metastatic lung tumors. Since metastatic lung tumors are not readily accessible to intratumoral drug delivery, parenteral drug administration was analyzed. Therapeutic effects of 1V270 were evaluated in three murine syngeneic tumor models: 4T1 breast cancer, B16 melanoma, and Lewis lung carcinoma (LLC). The results showed that a single systemic dose of 1V270 reduced tumor lung colonization in all three models tested. Systemic 1V270 therapy activated local innate immune cells, including natural killer (NK) cells and antigen-presenting dendritic cells (DCs). T cell receptor (TCR) repertoire analyses revealed that 1V270 therapy induced tumor-specific oligoclonal cytotoxic T cells, that were shared by different mice, and that suppressed the growth of metastatic tumors. Antimetastatic effects of 1V270 were also achieved by intranasal (i.n.) drug administration. These document that both i.n. and i.p. administration of a phospholipid-conjugated TLR7 agonist can safely induce tumor-specific cytotoxic T cell responses in pulmonary metastatic cancer and that peripheral T cell repertoire analysis may be used to monitor the effects of therapy. These observations support the concept that an immunomodulatory drug and TCR repertoire analysis can be applied for monitoring prognosis of metastatic lung cancer.

Results

Systemic Administration of 1V270 Inhibits Spontaneous Lung Metastasis in a CD8$^+$-Dependent Manner in a Murine 4T1 Orthotopic Breast Cancer Model. We have demonstrated that 1V270 induces tumor-specific adaptive immune responses when administered intratumorally (15, 16). However, recent reports claim that TLR7 activation in the lung can promote primary tumor growth (19, 20). The 4T1 mouse breast cancer cell line has been shown to be poorly immunogenic and highly metastatic, mimicking triple-negative breast tumor in humans. Accordingly, this model is commonly used for evaluation of new therapies for advanced-stage disease. Thus, we examined whether systemic 1V270 therapy would also promote tumor-specific adaptive T cell responses and if such responses could restrain pulmonary metastatic disease using the 4T1 breast cancer model. For this purpose, we employed the murine 4T1 breast cancer model that exhibits characteristics similar to the human disease, in which orthotopically implanted tumor cells spontaneously metastasize to the lung (23).

4T1 cells (5×10^5) were inoculated into the fourth mammary pads on day 0, and 1V270 (20, 80, or 200 μg per injection) was injected i.p. twice a week for 3 wk, starting on day 7 (Fig. 1*A*). Both the primary tumor volumes and the number of lung metastases were evaluated on day 27. Systemic 1V270 therapy decreased the number of lung metastases (Fig. 1*B*). However, the i.p. administration did not retard tumor growth at the primary sites of implantation, suggesting that rapid tumor growth could overcome immune restraints (*SI Appendix*, Fig. S1*A*).

To study the possible involvement of cytotoxic T cell immune responses in the antimetastatic effects of 1V270, CD8$^+$ cells were depleted with monoclonal antibodies (mAbs) before treatment with the TLR agonist (Fig. 1*C* and *SI Appendix*, Fig. S1*B*). In both the 1V270-treated and the vehicle-treated control mice, the number of lung nodules increased significantly ($P < 0.05$) after CD8$^+$ cell depletion (Fig. 1*C*). As expected, CD8$^+$ cell depletion did not alter the brisk tumor growth at the primary sites in the mammary glands (*SI Appendix*, Figs. S1*C* and S2).

I.p. Administration of 1V270 Induces Tumor-Specific CD8$^+$ T Cells in an i.v. Metastatic Model of 4T1 Breast Cancer. We used i.v. lung metastasis models to evaluate in more detail the immune response to circulating tumor cells induced by 1V270 therapy. Each animal received 2×10^4 4T1 cells directly in the tail vein on day 0, and the number of lung nodules were counted on day 21 (Fig. 2*A*). Similar to the results after orthotopic tumor inoculation, 1V270 inhibited lung metastasis in a dose-dependent manner, with the lowest effective dose being 20 μg (Fig. 2*B*). A subsequent study indicated that a single administration of 1V270 was sufficient to inhibit lung metastasis and that 1V270 had to be given 1 d before the tumor inoculation, which is important for maximal drug effects in this quickly developing lung metastasis model (Fig. 2*C*). 1V270 therapy also significantly prolonged the survival (Fig. 2*D*).

To examine the role of CD8$^+$ T cells after i.p. 1V270 treatment, mediastinal lymph node (mLN) cells, splenocytes, and lung tissues were analyzed in the i.v. metastasis model on day 21 (Fig. 2 *E* and *F*). Activation of CD8$^+$ T cells was assessed by intracellular staining for granzyme B and IFN-γ (IFNγ). Significantly higher percentages of granzyme B and IFNγ-positive CD8$^+$ T cells were detected in the 1V270-treated mice ($P < 0.05$, Fig. 2 *E* and *F*). Histological analysis revealed a higher infiltration of CD45$^+$CD3$^+$ cells in the pulmonary tumor microenvironment of 1V270-treated mice in comparison with those of vehicle-treated mice (Fig. 2*G*). The tumor-specific effector function of the CD8$^+$ cells was further evaluated by ex vivo cytotoxic T cell assays (Fig. 2*H*). Briefly, splenic CD8$^+$ T cells from 1V270-treated or vehicle-treated mice were cultured with antigen (4T1 tumor cell lysates) and IL-2, and then were incubated with carboxyfluorescein succinimidyl ester (CFSE)-labeled tumor cells. CD8$^+$ T cells from 1V270-treated mice showed significantly higher tumor-specific cytotoxicity at an effector to target cell ratio of 16:1 ($P < 0.05$, Fig. 2*H*). These results demonstrated that a single administration of systemic 1V270 therapy can inhibit lung colonization by tumors in a CD8$^+$

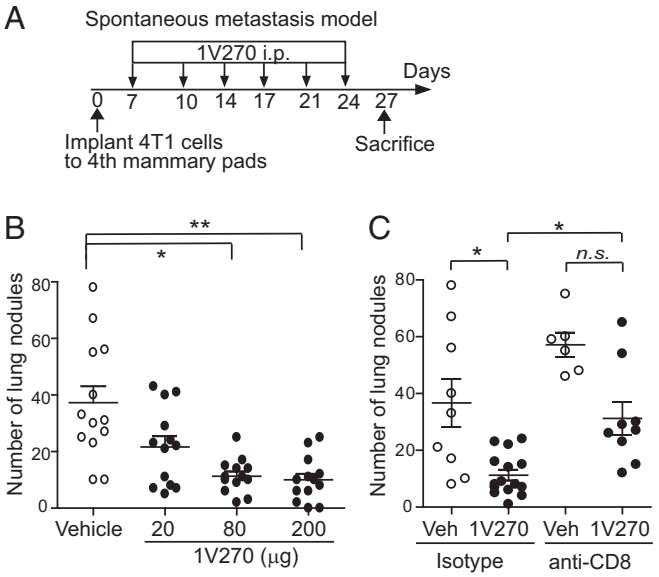

Fig. 1. Systemic administration of 1V270 inhibits lung metastasis in the 4T1 murine syngeneic breast cancer model in a CD8$^+$ T cell-dependent manner. (*A*) Protocol of spontaneous metastasis model. 4T1 cells (5×10^5) were inoculated in both fourth mammary pads of BALB/c mice ($n = 13$ per group). 1V270 (20, 80, or 200 μg per injection) was i.p. administered on days 7, 10, 14, 17, 21, and 24. (*B*) The numbers of lung nodules were counted by staining with India ink after harvesting lungs on day 27. (*C*) The mice ($n = 6$–15 per group) were orthotopically implanted with 4T1 cells and i.p. treated with 1V270 (20 μg per injection) as shown in *A*. CD8$^+$ cells were depleted by administration of anti-CD8 or isotype mAbs on days 5, 8, 11, 16, 19, and 23. The numbers of lung nodules were counted on day 27. Each dot indicates an individual mouse and horizontal and vertical bars indicate means ± SEM. Data shown are pooled from two independent experiments. *$P < 0.05$, **$P < 0.01$ by Kruskal–Wallis test with Dunn's post hoc test comparing treatment groups against vehicle group. n.s., statistically not significant.

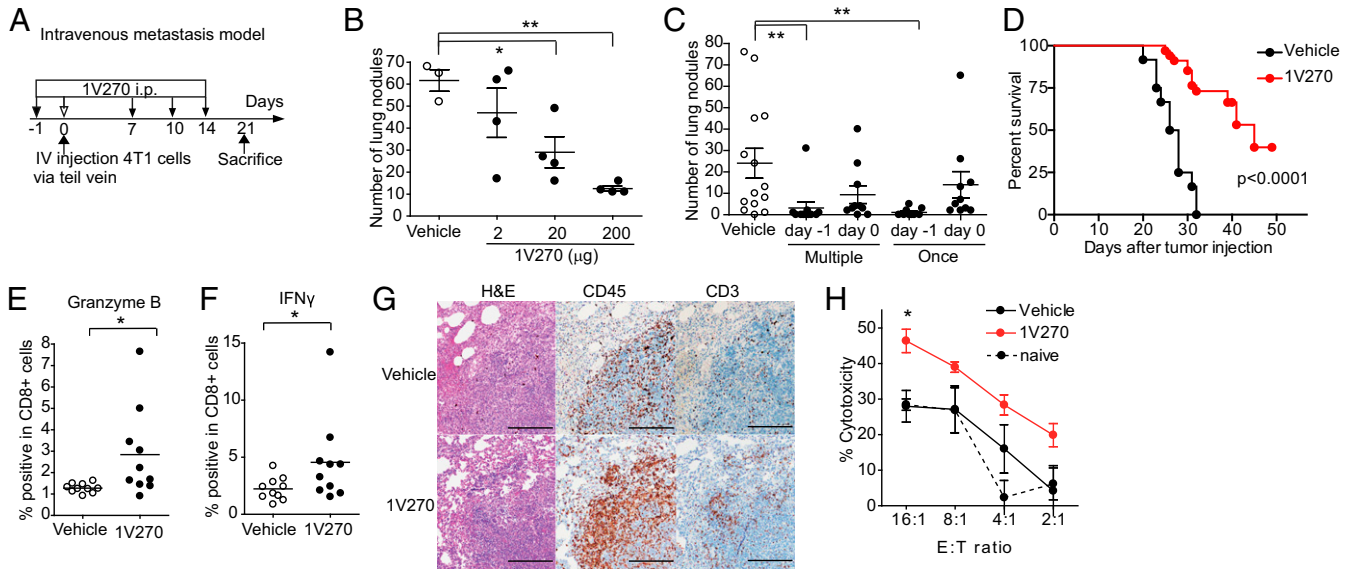

Fig. 2. Systemic administration of 1V270 induces tumor-specific CD8$^+$ T cells. (*A*) Protocol of I.V. metastasis model. (*B*) BALB/c mice (n = 8–15 per group) were i.v. injected with 4T1 cells (2×10^4) on day 0. 1V270 (2, 20, or 200 μg per injection) was i.p. administered on days −1, 7, 10, and 14. The numbers of lung nodules were counted on day 21. (*C*) 1V270 (200 μg per injection) was i.p. administered on days −1 or 0 followed by days 7, 10, and 14 where indicated. The numbers of lung nodules were counted on day 21. Each dot indicates an individual mouse and horizontal and vertical bars indicate means ± SEM. *$P < 0.05$, **$P < 0.01$ Kruskal–Wallis test with Dunn's post hoc test comparing treatment groups against vehicle group. (*D*) Mice were euthanized when they became moribund, lost more than 15% body weight, or the primary tumor developed necrosis. The survival data were analyzed by log-rank test ($P < 0.0001$). Data shown are pooled from three independent experiments showing similar results. (*E–H*) BALB/c mice (n = 10 per group) were treated with 1V270 (200 μg per injection) on day −1 and 4T1 cells were inoculated on day 0. (*E* and *F*) Three weeks later, mLNs cells were stained for CD3 and CD8. Intracellular granzyme B (*E*) and IFNγ (*F*) were analyzed by flow cytometry. Data are representative of two independent experiments showing similar results. *$P < 0.05$, by the Mann–Whitney U test comparing the 1V270 treatment groups against the vehicle-treated group. (*G*) Histological analysis of lungs on day 21. Representative images of H&E staining, and immunohistochemical staining for CD3 and CD45. (Scale bar: 100 μm.) (Original magnification: 200×.) (*H*) Tumor-specific cytotoxicity was examined using 4T1 cells as target cells and BALB/3T3 cells as irrelevant target cells. The splenocytes incubated with 4T1 cell lysate and IL-2 were cocultured with 4T1 and BALB/3T3 cells at 16:1 and 2:1 effector to target cell ratios (E:T), respectively, for 16 h. The percent specific killing was calculated. Data were analyzed by two-way ANOVA using a Bonferroni post hoc test comparing treatment groups against vehicle group. *$P < 0.05$. Data are representative of three independent experiments showing similar results.

cell-dependent manner and that the administration of 1V270 promotes adaptive CD8$^+$ immune responses against tumor cells.

Tumor-Infiltrating T Cells in 1V270-Treated Mice Show High Clonalities and Intraindividual and Interindividual Commonality by TCR Repertoire Analysis. Increased clonality of CD8$^+$ T cells has been associated with both a positive clinical outcome and immune-related adverse events after immune checkpoint therapy (24, 25). Other studies have also indicated that clonal expansion of tumor-specific T cells is a biomarker for suppression of tumor growth (26, 27). We have reported that intratumoral treatment with 1V270 induces local expansion of a systemic dispersion of oligoclonal tumor-specific T cells by TCR repertoire analysis using next generation RNAseq methodology (16). Thus, it was important to determine whether systemic 1V270 therapy also induced oligoclonal expansion of tumor-specific T cells.

To validate that 1V270 therapy induced tumor-specific adaptive immune responses, we monitored the growth of secondarily challenged tumors following 1V270 treatment. The mice treated with 1V270 using the i.v. metastasis protocol were orthotopically rechallenged with 4T1 cells on day 21 (Fig. 3*A*). We compared the growth of rechallenged tumors between 1V270-treated mice that were not exposed to the tumor (no-tumor exposed), and 1V270-treated and tumor-exposed mice (Fig. 3*A*). Naïve mice were also orthotopically injected with tumor cells as a positive control. The tumor growth was significantly impaired in the mice treated with 1V270 and exposed to the tumor cells compared with the naïve mice or 1V270-treated no-tumor–exposed mice ($P < 0.01$, Fig. 3*B*). As expected, there was no difference in the tumor growth between naïve mice and 1V270-treated no-tumor exposure mice (Fig. 3*B*). To examine whether tumor-specific T cells were recruited into the microenvironment of the secondary challenged tumor, CD8$^+$ cells in the tumor infiltrating lymphocytes (TILs) were analyzed by flow cytometry (Fig. 3*C*). Threefold higher numbers of CD8$^+$ T cells were detected in the TILs from the 1V270-treated and tumor-exposed mice, compared with the 1V270-treated and no-tumor–exposed mice ($P < 0.05$, Fig. 3*C*). In this experiment, more than 80% of CD8$^+$ T cells in TILs were positive for PD-1 (Fig. 3*C*), indicating that they were exposed to antigen (tumor cells) and activated (28).

To examine clonal specificity of tumor-specific T cells, CD8$^+$ cells were isolated from the spleens and the TILs of secondarily challenged tumors after initial 1V270 therapy. The TCR repertoires were assessed by next generation RNA sequencing of both TCRα and TCRβ genes as previously described (29). The clonality indices of CD8$^+$ T cells in TILs, as assessed by 1-Shannon index, were negatively correlated with the volumes of the secondarily challenged tumors only in the mice treated with 1V270 and exposed to tumor cells (Pearson's correlation coefficient, $r^2 = 0.97$, $P = 0.015$, Fig. 3*D* and *SI Appendix*, Fig. S3*A*). When the frequencies of commonly shared TCR clones between TILs and splenocytes were evaluated using a binary similarity measure (Baroni-Urbani and Buser overlap index, BUB index) (30), the 1V270-treated and tumor-exposed mice showed significantly higher BUB indices than the control no-tumor–exposed mice ($P < 0.05$, Fig. 3*E*). The clonotypes in individual tumor-exposed mice showed a higher similarity in the 1V270-treated group in comparison with the no-tumor–exposed group (Fig. 3 *F* and *G*). Indeed, 31 TCRα and 11 TCRβ clonotypes were shared by three or more individuals in the tumor-exposed group, but only five TCRα

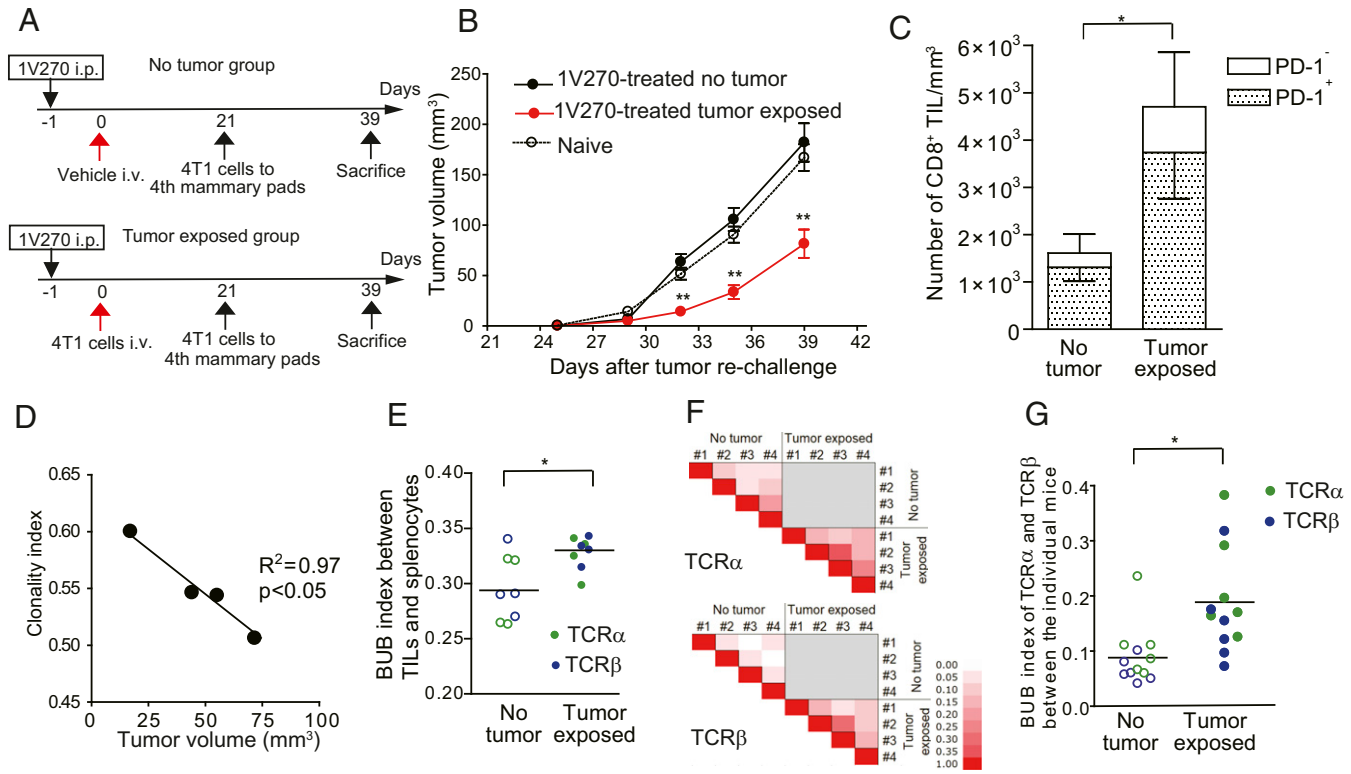

Fig. 3. Tumor infiltrating T cells in 1V270-treated mice show high clonalities and increased frequency of intraindividual and interindividual common clones. (*A*) Experimental protocols of the secondary challenge studies. Two groups of BALB/c mice ($n = 5$ per group) were i.p. treated with 1V270. One cohort of mice was i.v. injected with 4T1-GLF cells (2×10^4) on day 0, and tumor growth in the lungs was monitored by IVIS on day 20. Another cohort did not receive i.v. tumor injection (no-tumor–exposed mice). Naïve BALB/c mice served as controls. 4T1 cells were orthotopically inoculated on day 21. (*B*) Tumor growth was measured with a caliper and calculated using the formula: volume (mm^3) = $(\text{width})^2 \times \text{length}/2$. (*C*) TILs were isolated from the secondarily challenged tumor on day 39 and stained for $CD8^+$ T cells ($CD3^+CD8^+$) and PD-1. The numbers of tumor-infiltrating $CD8^+$ T cells were expressed per tumor volume (mm^3). Data are representative of two independent experiments showing similar results. Results were analyzed by the Mann–Whitney *U* test comparing the 1V270 treatment groups against the vehicle treated group. $^{**}P < 0.01$. (*D*–*G*) TCR repertoire of $CD8^+$ T cells from TILs and splenocytes were examined. (*D*) The clonality index (1 − normalized Shannon index) of $CD8^+$ T cells infiltrating to the left side of the secondarily challenged tumor was plotted against tumor volume in the tumor-exposed mice. Correlation between the clonality index and the tumor volume was evaluated by Pearson's method ($R^2 = 0.97$, $P < 0.05$). (*E*) BUB overlap index of $CD8^+$ T cells TCRα (green) or TCRβ (blue) between TILs and splenocytes in each individual. Higher BUB index shows higher similarity of TCR repertoire between TILs and splenocytes. Each point shows the BUB index of individual mouse. (*F*) Heat map of BUB overlap index of TCRα or TCRβ in the same group. The color scale bar on the *Left* shows that white is zero and red is 1. (*G*) BUB overlap index of TCRα (green) or TCRβ (blue) between individual mice was plotted. Statistical analysis was performed by the Mann–Whitney *U* test for comparing two groups. $^{*}P < 0.05$. Each point represents the BUB overlap index of TCRα or TCRβ between pairs of individual mice in the same groups.

clonotypes were shared in the no-tumor–exposed group (*SI Appendix*, Fig. S3*B*). The frequency of shared clones was significantly higher in tumor-exposed mice than in no-tumor–exposed mice (*SI Appendix*, Fig. S3*C*). These experiments showed that 1V270 therapy increased clonality of $CD8^+$ T cells and the frequency of intraindividual and interindividual shared clones, which correlated with the growth inhibition of secondarily challenged tumors.

DCs in the Lungs and Draining Lymph Nodes Are Activated, and $CD8^+$ T Cells Are Recruited to the Draining Lymph Nodes Following 1V270 Therapy. Previously, we demonstrated that 1V270 activates antigen presenting cells (APCs) and promotes cross-presentation of antigen to $CD8^+$ T cells (31). Since the 1V270 therapy induced a tumor-specific $CD8^+$ T cell response in the 4T1 model, we evaluated whether the therapy activated APCs in the lungs and/or in the draining lymph nodes. BALB/c mice were i.p. administered with 1V270 on day −1 and 4T1 cells were injected on the next day (day 0). The DC populations were examined in the draining mLNs and lungs on day 7 after the tumor injection. In the 1V270-treated mice, a population of $CD11c^+$ DCs was increased in both mLNs and the lungs ($P < 0.01$, Fig. 4*A* and *SI Appendix*, Fig. S4 *A* and *B*). Furthermore, the frequencies of $CD11c^+$ cells expressing costimulatory molecules (CD80 or CD86) were also significantly increased at both sites ($P < 0.01$, Fig. 4*B* and *SI Appendix*, Fig. S4*C*). The activation of DCs was accompanied by the recruitment of $CD8^+$ T cells with memory and naïve phenotypes (Fig. 4*C*): central memory $CD8^+$ T cells ($CD8^+CD44^+CD62L^+$), effector memory $CD8^+$ T cells ($CD8^+CD44^+CD62L^-$), and naïve $CD8^+$ T cells ($CD8^+CD44^-CD62L^+$) ($P < 0.05$ and $P < 0.01$, Fig. 4*C*). These findings demonstrate that 1V270 activated local APCs and promoted their maturation, leading to expanded $CD8^+$ T cell subsets.

1V270 Treatment Activates Innate Immunity and Inhibits Lung Colonization by Tumor Cells in an NK-Cell Dependent Manner. In the i.v. metastasis model, the administration of 1V270 one day before i.v. injection of tumor cells was required to restrain lung colonization. Since adaptive immune responses require several days to develop, this observation indicated that one or more innate immune cell types in the lung mediated the early therapeutic effect. To enable the monitoring of the detailed kinetics of the colonization process of 4T1, cells expressing both green fluorescent protein (GFP) and luciferase (4T1-GLF) were prepared using lentivirus vectors (32). Subsequently, tumor implantation and growth were monitored using an IVIS Spectrum in vivo imaging system. In both vehicle- and 1V270-treated mice, tumor cells accumulated in the lungs quickly after the injection (at 0 h, Fig. 4*D* and *SI Appendix*,

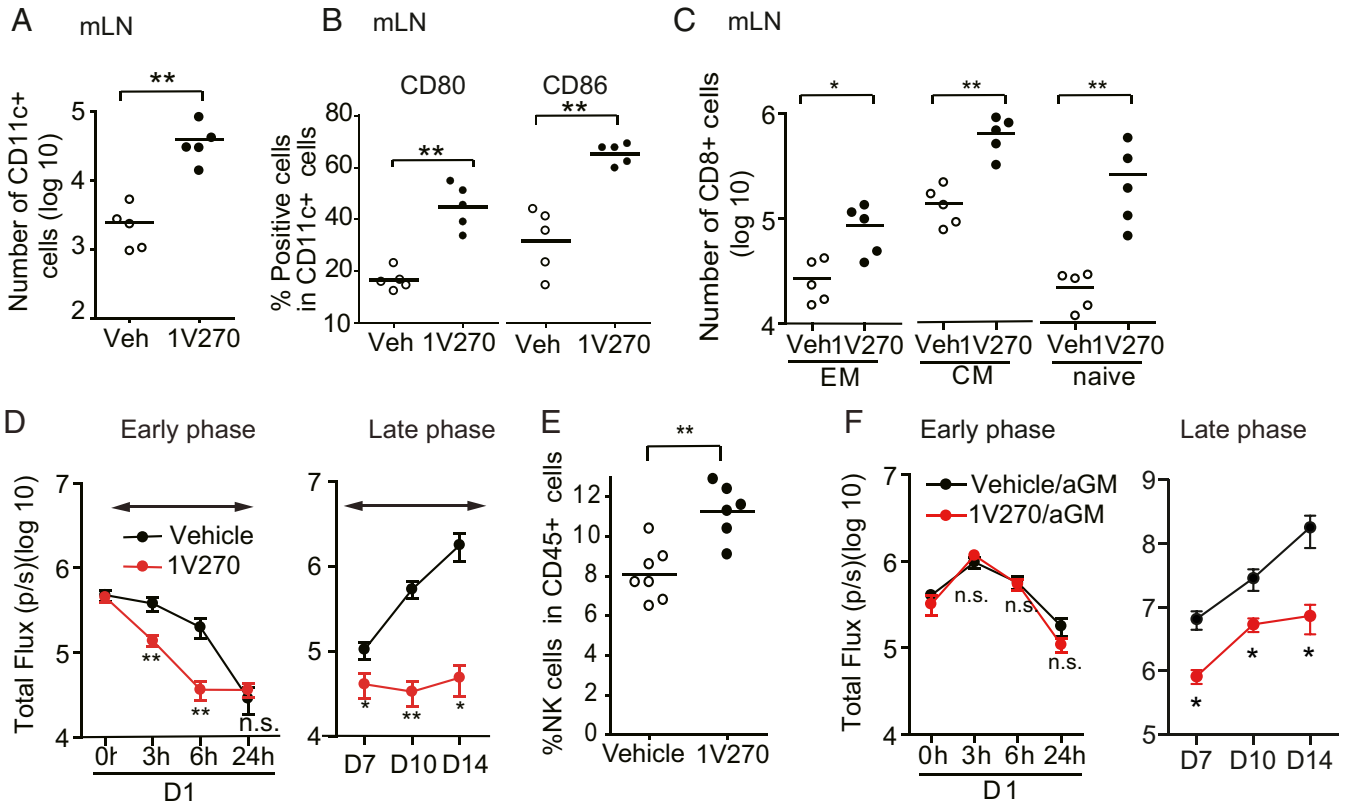

Fig. 4. Innate immune cells, NK cells, and DCs are activated following 1V270 therapy and contribute to antimetastatic effects. (*A–C*) Systemic administration of 1V270 activates DCs and increases $CD8^+$ cell recruitment in the lung draining lymph node. (*A*) BALB/c mice ($n = 5$ per group) were treated with 1V270 on day −1 and then tumor cells were i.v. administered on day 0. Seven days later, mLN cells were stained for DCs (DC; $CD45^+CD11c^+$MHC classII$^+$). (*B*) DCs were further stained for CD80 and CD86. (*C*) The mLN cells were also stained for central memory $CD8^+$ T cells ($CD3^+CD8^+CD44^+CD62L^+$), effector memory $CD8^+$ T cells ($CD3^+CD8^+CD44^+CD62L^-$), and naïve $CD8^+$ T cells ($CD3^+CD8^+CD44^-CD62L^+$). Each dot indicates an individual mouse and horizontal bars indicate means ± SEM. Data are representative of three independent experiments showing similar results. $^*P < 0.05$, $^{**}P < 0.01$ by Mann–Whitney *U* test comparing the individual groups. (*D–F*) In vivo imaging analyses using GLF-expressing 4T1 cells (4T1-GLF). (*D*) BALB/c mice ($n = 14–15$ per group) were i.p. administered with 200 μg of 1V270 or vehicle. On the next day, 2×10^4 4T1-GLF cells were i.v. injected through the tail vein. Tumor signals were quantified by IVIS. Data (mean ± SEM) were pooled from three independent experiments showing similar results. $^*P < 0.05$, $^{**}P < 0.01$ by two-way ANOVA using a Bonferroni post hoc test comparing treatment groups against the vehicle group. (*E* and *F*) NK cells recruited by 1V270 therapy prevent colonization of 4T1 cells. (*E*) BALB/c mice ($n = 6–7$ per group) were treated with 1V270 (200 μg per injection) on day −1 and then tumor cells were i.v. administered on day 0. On day 7, lung cells were stained for NK markers ($CD45^+CD3^-NKp46^+CD49^+$) and analyzed by flow cytometry. Mann–Whitney *U* test was used to compare treatment groups against the vehicle group. $^{**}P < 0.01$. (*F*) Lung tumor signal in early and late phases following NK cell depletion. 1V270-treated BALB/c mice ($n = 10$ per group) received 4T1 cells i.v. on day 0. NK cells were depleted by administration of anti–asialo-GM1 antibody (aGM, 50 μg per injection) on day −4, and −1. Tumor signals were analyzed as described above. Data (mean ± SEM) were pooled from two independent experiments showing similar results. $^*P < 0.05$ by two-way ANOVA using Bonferroni post hoc test was used to compare treatment groups against the vehicle in the first 24 h. n.s., not significant.

Fig. S5). Thereafter, the signals progressed in two phases: They declined almost to baseline within the first 24 h (the early phase) and then increased after day 7 (the late phase). The 1V270 treatment significantly suppressed the tumor signals both in the early ($P < 0.01$ on 3 h and 6 h) and late phases ($P < 0.05$ on days 7, 10, and 14).

To identify the types and functions of innate immune cells recruited into the lung following 1V270 administration, the mice were injected with 1V270 on day −1, 4T1 cells were i.v. administered on day 0, and the lung cells were isolated on day 7 after the tumor injection. A single-cell suspension of lung cells was stained for NK cells and MDSCs and analyzed by flow cytometry (*SI Appendix*, Fig. S6 and Table S1). Significantly increased populations of NK cells and monocytic-MDSC were recruited to the lungs following 1V270 treatment, in comparison with the vehicle treatment ($P < 0.01$, Fig. 4*E* and *SI Appendix*, Fig. S6*C*). However, similar populations of granulocytic (PMN)-MDSCs accumulated in the lungs in the 1V270-treated mice compared with those of the vehicle-treated animals (*SI Appendix*, Fig. S6*C*).

NK cells can be activated directly by TLR7 agonists, and indirectly by type I IFN that is secreted from accessory DCs (33, 34). To examine the role of NK cells in the early therapeutic efficacy of 1V270, this cell type was depleted by treatment with anti-asialo GM1 polyclonal antibody (35). Over 90% of NK cells were depleted by antibody injection on days −4, −1, 3, and 10 (*SI Appendix*, Fig. S7 *A* and *B*). IVIS analysis showed that lung colonization by tumor cells in 1V270-treated NK cell-depleted mice during the early phase developed similar to that in vehicle-treated mice (Fig. 4*F* and *SI Appendix*, Fig. S7*C*). In the later phase, the kinetic analysis using IVIS showed that 1V270 therapy significantly suppressed lung tumor signals (Fig. 4*F*). These data indicated that mice were refractory to 1V270 therapy in the early phase following NK-cell depletion, while 1V270 therapy was able to significantly suppress lung tumor colonization at later time points.

Intranasal Administration of 1V270 Is also Effective in Preventing Metastasis and in Inducing Antitumor Immunity. Although the i.p.

administration of 1V270 could prevent the lung metastasis, it did not alter the primary tumor growth in the mammary glands. To understand this finding, we studied whether there is any preferential immune cell activation in the regional lymph nodes of the lungs following i.p. 1V270 treatment. DC activation in mediastinal, cervical, and inguinal lymph nodes was examined following i.p. 1V270 administration (*SI Appendix*, Fig. S8*A*). The number of DCs at mediastinal lymph nodes peaked on day 7 and declined to the baseline by day 21 (*SI Appendix*, Fig. S8*A*). An increased population of DCs was observed only in the mediastinal lymph nodes (*SI Appendix*, Fig. S8*B*). The activation of DCs was monitored by CD80 and CD86 expression using flow cytometric assay (*SI Appendix*, Fig. S8 *C* and *D*). A higher population of activated $CD80^+$, or $CD86^+$-positive cells in the gated $CD11c^+$ population, was observed only in the mediastinal, but not other lymph nodes (*SI Appendix*, Fig. S8 *C* and *D*). Furthermore, the increased number of activated DCs was associated with higher numbers of activated PD-1^+ $CD8^+$ T cells (*SI Appendix*, Fig. S8 *E* and *F*). These data suggest that i.p. administration of 1V270 activate the lung draining lymph nodes and essentially act as a delivery system to the pulmonary tissues. These results further let us hypothesize that direct intrapulmonary administration of 1V270 could prevent lung metastasis.

We previously demonstrated that i.n. administration of 1V270 activates nasal and lung APCs, without causing systemic cytokine release (14). Therefore, we examined whether i.n. 1V270 treatment could impair tumor growth in the i.v. metastasis model (Fig. 5*A*). 1V270 (20 or 200 μg per 50-μL dose) was i.n. delivered on days −3, −1, 3, 7, and 10 relative to the 4T1 tumor cell injection (day 0) (Fig. 5*A*). Intranasally administrated 1V270 inhibited the number of lung nodules in a dose-dependent manner (Fig. 5*B*).

We next examined whether i.n. administration of 1V270 could induce tumor-specific adaptive immune responses similar to the effects of systemic administration. Mice were treated with i.n. 1V270 (200 or 500 μg per 50 μL) and then received 4T1 cells by the i.v. route. The surviving mice on day 21 were orthotopically rechallenged with tumor cells. The rechallenged tumor growth was significantly inhibited in the mice that were i.n. treated with 1V270 (Fig. 5*C*). The tumors grew similarly in naïve mice when the mice received 1V270 treatment intranasally without tumor cell injection (Fig. 5*C*). A higher number of $CD8^+$ T cells and PD-$1^+$$CD8^+$ T cells were detected in TILs from i.n. 1V270-treated mice exposed to the tumor cells, in comparison with 1V270 treated without tumor exposure or naïve mice (Fig. 5*D*). These findings indicate that i.n. delivery of 1V270 effectively inhibited lung metastasis by inducing tumor-specific adaptive immune responses, similar to systemic 1V270 therapy.

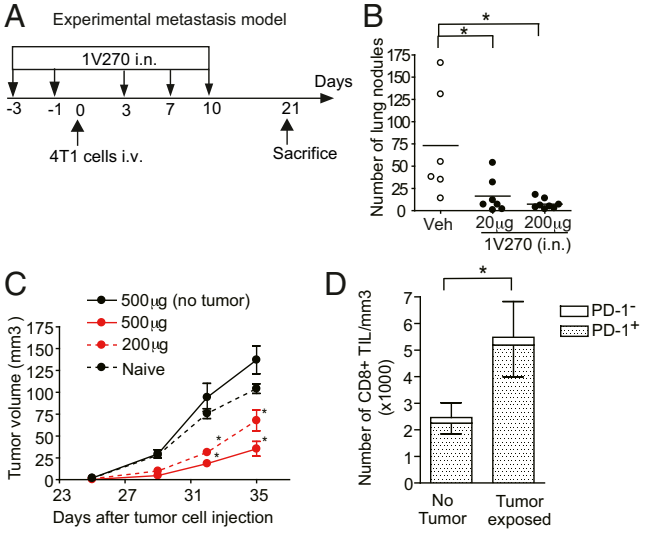

Fig. 5. Intranasally administered 1V270 inhibits pulmonary colonization in experimental metastasis models. Protocol for testing the therapeutic efficacy of i.n. treatment with 1V270 in i.v. metastasis model. (*A*) BALB/c mice ($n = 6$–8 per group) were i.n. administered with 1V270 (20 or 200 μg) or vehicle on days −3, −1, 3, 7, and 10. 4T1 cells were i.v. injected on day 0. (*B*) The numbers of lung nodules were counted on day 21. *$P < 0.05$ calculated by Kruskal–Wallis test with Dunn's post hoc test. (*C*) Intranasal 1V270 therapy attenuated the growth of secondarily challenged tumors. BALB/c mice ($n = 5$) were i.n. treated with 200 μg of 1V270 on days −3, −1, 3, 7, and 10. 4T1 cells were injected on day 0. On day 21, the surviving mice were orthotopically inoculated with 4T1 cells and tumor growth was monitored. The mice treated with 1V270 without i.v. tumor cell injection served as controls. (*D*) TILs were isolated from the secondarily challenged tumor, and the numbers of $CD8^+$ T cells and PD-1–expressing $CD8^+$ T cells were analyzed by flow cytometric assay. Data were analyzed by the Mann–Whitney *U* test comparing two groups. *$P < 0.05$. Data are representative of two independent experiments showing similar results.

Antimetastatic Effects of 1V270 Were Observed in Murine Syngeneic Melanoma and Lung Carcinoma Models. To evaluate whether the 1V270 therapy can be effective in other cancer types, we employed two additional murine syngeneic metastasis models: B16 melanoma and LLC. Luciferase and GFP-expressing cells (B16-GLF and LLC-GLF) were prepared using a lentivirus vector for in vivo imaging analysis. Mice received systemic 1V270 treatment on day −1, and then B16-GLF and LLC-GLF cells were i.v. administered on day 0. In both metastasis models, 1V270 inhibited lung metastasis by day 14 (Fig. 6 *A* and *E*) and prolonged mouse survival (Fig. 6 *B* and *F*).

Safety Assessment of 1V270 Therapy. Safety is a critical problem in cancer immunotherapy. We performed two studies to determine the maximum tolerated dose (MTD) of 1V270 in two strains of mice, C57BL/6 and CD-1. The MTD was 71 mg/kg in C57BL/6 and between 75 and 85 mg/kg in CD-1 mice. The effective dose of this compound that prevents the lung metastasis was about 0.8 mg/kg (20 nmol/25 g of mouse) in the orthotopic metastasis model. Thus, the MTD was 88 times higher than the effective dose, indicating that this compound has a wide therapeutic window. We have reported previously that small molecule TLR7 ligands induce an anorexic response in mice, mainly attributable to mast cell degranulation (36). Reduced body weight the day after administration of 1V270 was observed in wild-type mice after i.p. or i.v. injection of 1V270 at the MTD (*SI Appendix*, Fig. S9*A*). Such body weight loss was not observed in mice receiving 20 or 200 nmol/kg (0.8 or 8 mg/kg) 1V270 (*SI Appendix*, Fig. S9*B*). Furthermore, repeated dosing did not cause significant body weight loss in the 4T1 i.v. metastasis model (*SI Appendix*, Fig. S9*C*). Of note, TLR7-deficient mice were refractory to body weight loss following 1V270 injection, indicating that the body weight loss is an on-target adverse effect (*SI Appendix*, Fig. S9*D*).

TLR7 agonists are known to induce reversible lymphopenia (37). This phenomenon is type I IFN-dependent as type I IFN receptor-deficient mice were refractory to this effect (37). To test whether the effective doses of 1V270 may cause these adverse effects, we assessed an additional experiment to test complete blood counts (CBC) and other serum chemistries after 1V270 administration. When the mice received 0.8 or 8 mg/kg (20 and 200 nmol/25 g) 1V270 via i.p. route, only a mild increase of neutrophils and decrease of lymphocytes were observed (*SI Appendix*, Table S2). Similarly, an effective dose 1V270 did not increase the chemistry parameters for liver, pancreas, and kidney function (*SI Appendix*, Table S2). We also screened for off-target binding of 1V270 to GPCRs, ion channels, transporters, and kinase and nonkinase enzymes (Eurofins Pharma). 1V270 only showed nonspecific weak binding to only one receptor (androgen

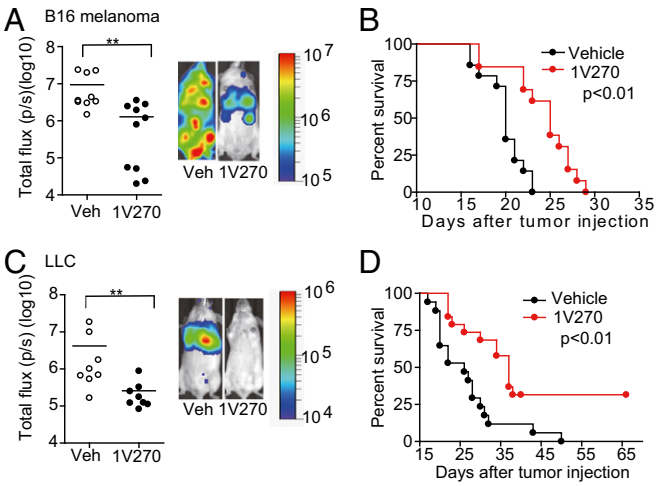

Fig. 6. Systemic 1V270 therapy effectively inhibits lung colonization in melanoma and LLC models. Therapeutic effects of 1V270 were evaluated in i.v. metastatic models of B16 melanoma (*A* and *B*) and LLC (*C* and *D*). B6-albino mice (n = 8–10) (*A* and *C*) and C57BL6 wild-type mice (n = 15–20) (*B* and *D*) were i.p. administered with 200 μg of 1V270 or vehicle. Next day, 5×10^5 B16-GLF cells (*A*) or 1×10^6 LLC-GLF cells (*C*) were i.v. administered. (*A* and *C*) The tumor signals were quantified by IVIS at day 14. The data are displayed as a radiance on a color bar with a range of 1×10^5 to 1×10^7 (*A*) or 1×10^4 to 1×10^6 (*C*). (*B* and *D*) The mice were monitored daily and were euthanized upon reaching the criteria according to UCSD Institutional Animal Care and Use Committee guidelines. The survival data were analyzed by log-rank test. Data were analyzed by Living Image software and were pooled from two independent experiments showing similar results. Each dot indicates an individual mouse and horizontal bars represent means. Statistical differences were analyzed by the Mann–Whitney *U* test comparing 1V270 treatment groups against the vehicle. $^{**}P < 0.05$.

receptor, *SI Appendix*, Table S3). Because of its wide therapeutic window and a minimal off target binding profile, 1V270 is safe for clinical use.

Discussion

In patients with an advanced stage of cancer, the development of metastasis is almost inevitable since the metastatic niches are seeded with tumor cells long before clinical presentation (38). The ability of immune-checkpoint inhibitors to reactivate tumor-specific cytotoxic T cells provided evidence that immunotherapy can overcome these limitations, at least in some patients. Thus, there is an unmet medical need for additional agents that can increase the frequency of cytotoxic T cells at metastatic sites. We demonstrated that a small molecule TLR7 agonist-phospholipid conjugate, 1V270, could activate innate immune cells in the lungs and prevent lung metastasis in the 4T1 mouse breast cancer model, which resembles immunogenic triple-negative breast tumors in humans.

Because each immunotherapy type exploits a distinct biological mechanism, biomarkers that predict efficacy and adverse effects are required (39). We demonstrated that systemic 1V270 treatment induced cytotoxic tumor-specific $CD8^+$ T cells, as assessed by both in vitro tumor-specific cytotoxicity assays and tumor rechallenge experiments. TCR repertoire analyses of TILs in the secondarily challenged tumors indicated that 1V270 therapy strongly increased T cell clonality. The levels of clonality negatively correlated with the tumor volumes of secondarily challenged tumors. Of interest, the clonal similarity between tumor infiltrating and splenic T cells was increased in 1V270-treated and tumor-exposed animals. A recent paper demonstrated that antitumor immune cells proliferate in the secondary lymphoid organs, including draining LNs and spleen, and can be detected in the peripheral blood during tumor rejection (40). These findings suggested that immune monitoring should be possible by analyzing the TCR repertoire of peripheral T cells.

Theoretically, the TCR repertoire might be diverse among individual tumor-bearing mice, although they share the same genetic background (41). In a chronic virus infection, patients develop common clones that interact with highly immunodominant antigens (42, 43). In our study, an eightfold higher number of shared clones in TILs was identified in the 1V270-treated and tumor-exposed group, compared with the no-tumor–exposed group. As increased frequency of shared clones suggested that the systemic 1V270 treatment may skew the TCR repertoire toward tumor-specific clones, that may recognize the same tumor antigens.

When administrated locally, synthetic TLR7 and TLR9 agonists are potent immune adjuvants, that can induce Th1 and cytotoxic T cell responses over a period of a week (16, 44). When given systemically, however, some TLR agonists can cause a cytokine release syndrome that could potentially enhance metastatic growth by stimulating either angiogenesis or the development of M2 macrophages (45, 46). Therefore, effective systemic TLR7 therapy must clearly demonstrate that CD8 responses are induced without toxicity to the host or adverse changes in the tumor microenvironment. Our data demonstrated that some monocyte lineage, myeloid derived suppressor cells (MDSCs) were recruited to the lung after 1V270 administration. Immature MDSCs have the ability to suppress antitumor T cell responses (47). Thus, we were concerned that systemic 1V270 treatment may promote tumor growth. However, other innate immune cells, including NK cells and DCs, were also recruited to the lung after 1V270 administration, as reported previously in other models using TLR ligands (48). The recruitment and activation of the NK cells impeded tumor lung colonization, indicating that the NK cells could overcome the suppressive function of MDSC recruited by 1V270 administration. Another concern in immunotherapy using TLR7 ligands is that stimulation of a tumor TLR7 pathway could promote growth and chemoresistance in some primary tumors expressing this receptor (19, 20). In our study, 4T1, B16, and LLC cells did not express TLR7 by quantitative RT-PCR (*SI Appendix*, Fig. S10). We, therefore, conclude that systemic and i.n. TLR7 treatment is an effective therapy for TLR7 negative tumors.

We reported that 1V270 inhibited the growth of small s.c. tumors when locally (intratumorally) injected (15, 16). In the 4T1 metastatic model, orthotopically implanted primary tumors in the mammary gland were unaffected by i.p. 1V270 treatment. To address this discrepancy, we evaluated DC activation in lung draining (mediastinal), cervical, and inguinal lymph nodes following i.p. 1V270 administration. Using CD80, and CD86 expression as activation markers, we identified that DCs only in the lung draining mediastinal lymph nodes were activated by i.p. 1V270, but DCs in other sites were not activated by the drug. The 1V270 TLR7 agonist spontaneously forms small (100–120 nm) liposomes that are efficiently taken up by phagocytic cells, which are then activated. We believe that the activated monocytes and DCs quickly reach the pulmonary tissues and mediastinal lymph nodes and are retained there. Hence, there is no systemic cytokine syndrome. Similarly, the therapeutic effects on the s.c. tumor depend on the development of an adaptive immune response in the draining lymph nodes, which takes up to 14 d, and is insufficient before that time to halt the tumor growth. Thus, 1V270 systemic (or intrapulmonary) administration of 1V270 may be particularly useful for immunotherapy of lung tumors, including both primary and metastatic lesions.

The experiments in which NK cells were depleted by administration of antiasialo GM1 suggested that the ability of the TLR7 phospholipid agonist to prevent early lung metastasis

depended on this cell type. The in vivo imaging studies in NK cell-depleted mice confirmed the critical role of NK cells in constraining early tumor colonization, thus allowing for the development of a specific CD8 T cell response in the later phases of metastasis.

Intratracheal administration of a low molecular weight TLR7 agonist (SM276001) was reported to suppress metastatic lung tumors (18). We demonstrated that a low molecular weight TLR7 agonist (SM360320) (1V136) induced high levels of systemic proinflammatory cytokines following parenteral and i.p. administration to mice and that conjugation of a TLR7 ligand to a phospholipid moiety could markedly reduce in vivo cytokine release (*SI Appendix*, Fig. S11) (13). Intranasally administered 1V270 induced local (lung) immune cell activation without inducing systemic cytokine release (14). These results prompted us to assess whether the drug might have an immunotherapeutic effect in pulmonary metastatic disease. Our data demonstrated that i.n. administration of 1V270 suppressed lung metastasis similar to parenteral inoculation (Fig. 5), suggesting that i.n. delivery might be clinically attractive for this drug.

In summary, we have demonstrated that single systemic administration of a phospholipid-conjugated TLR7 agonist inhibited lung metastasis in three different murine syngeneic models of human malignancy: 4T1 breast cancer, B16 melanoma, and LLC models. 1V270 is clinically acceptable because of a wide therapeutic window and a minimal off-target binding profile. The drug quickly activated NK cells in the lung and later induced a cytotoxic T cell response. These two different mechanisms, NK cell-mediated and tumor-specific adaptive T cell responses, were responsible for the early and late phases of tumor growth inhibition. The antitumor effects were achieved without significant systemic release of inflammatory cytokines following administration. Furthermore, 1V270 therapy induced oligoclonal $CD8^+$ T cell responses as determined by TCR repertoire analyses of both spleen and mediastinal lymh nodes. The emergence of shared T cell clones correlated with the development of adative immunity against tumor cells. These results suggest that TCR repertoire analyses may be used to guide clinical trials of TLR and other immunotherapies in patients with metastatic cancer.

Materials and Methods

Animals and Reagents. Wild-type female BALB/c mice, C57BL/6, and B6-albino mice were purchased from Jackson Laboratory. TLR7-deficient mice (C57BL/6 background) were kindly gifted by Shizuo Akira, Osaka University, Osaka, Japan and bled by University of California, San Diego (UCSD) Animal Care Program. The studies involving animals were carried out in strict accordance with the recommendations in the *Guide for the Care and Use of Laboratory Animals* of the National Institutes of Health (49). A small molecule TLR7 ligand (1V136, SM360320) and phospholipid-conjugated TLR7 agonist, 1V270, were synthesized in our laboratory as described previously and was formulated in 20% hydroxypropyl-β-cyclodextrin (13). Endotoxin levels of these drugs and other reagents were determined by Endosafe (Charles River Laboratory) and were less than 15 EU/mg.

Lung Metastasis Models. The 4T1 (mouse breast cancer cell line), B16 melanoma cell line, and LLC cell line and BALB/3T3 fibroblast (Clone A31, CLL163) were obtained from American Type Culture Collection. The cells were tested for murine pathogens and were confirmed negative before inoculation in mice. GLF-expressing 4T1, B16, and LLC cells were prepared as described previously (32). Two metastatic 4T1 models, spontaneous and i.v. metastasis models, were used in this study. The detailed protocols are described in the *SI Appendix, Supplementary Text*.

In Vivo Imaging Study of Lung Tumor Growth. GFP and luciferase (GLF)-expressing tumor cells (2×10^4 of 4T1-GLF, 5×10^5 of B16-GLF, and 1×10^6 of LLC-GLF) were i.v. injected into BALB/c mice for 4T1 models, B6-albino, or wild-type C57BL/6 for B16 melanoma or LLC models). To generate bioluminescence signals, D-luciferin (3 mg/100 μL per mouse) was injected i.p. 12–15 min before the image acquisition. Image data were acquired by 15 s exposure using the IVIS Spectrum and analyzed using the Living Image software, version 4.5.2 (PerkinElmer). We confirmed that the tumor signals in the lungs at day 10 correlated with the number of lung metastasis determined on day 21, as well as the overall survival (*SI Appendix*, Fig. S12).

Flow Cytometric Analysis. The cells were labeled by incubating with mixtures of antibodies at 4 °C for 30 min (*SI Appendix*, Table S1) to identify various cell types.

NK Cells and $CD8^+$ Cell Depletion in Vivo. Anti-asialo GM1 rabbit polyclonal antibody (Wako) or rabbit IgG polyclonal antibody (Millipore) was used for NK cell depletion. Mouse anti-CD8 (clone 2.43), and isotype control Ab (clone LFA-2) were used for $CD8^+$ cell depletion. We confirmed over 90% depletion of NK cells and $CD8^+$ cells using flow cytometry (*SI Appendix*, Figs. S1 and S6).

Ex Vivo Tumor-Specific Cytotoxicity Study. Tumor-specific cytotoxicity was examined using 4T1 cells as target cells and BALB/3T3 cells as irrelevant cells. BALB/c mice were treated with 1V270 (200 μg per injection) on day −1, and 4T1 cells were inoculated on day 0. Three weeks later, splenocytes were incubated with 4T1 cell lysate and 10 units/mL IL-2 for 3 d. 4T1 and BALB/3T3 cells were labeled with 2.5 μM and 0.25 μM CFSE, respectively, for 12 min at 37 °C and were mixed at 1:1 ratio. Splenocytes cultured for 3 d were then cocultured with 4T1 and BALB/3T3 cells at 16:1–2:1 effector to target cell ratio (E:T) for 16 h. The frequencies of 4T1 (CFSE high) and BALB/3T3 (CFSE low) cells were determined by flow cytometry, and the percent specific killing was calculated. Specific killing (%) = [1 − "Sample ratio"/"Negative control ratio"] × 100; "Sample ratio" = [4T1 (target)/BALB/3T3 (irrelevant)] value of each sample cocultured with splenocytes; "Negative control ratio" = [4T1 (target)/BALB/3T3 (irrelevant)] value cultured without $CD8^+$ T cells.

TCR Repertoire Analysis. $CD8^+$ T cells were isolated from single-cell suspensions of tumors, or spleens using mouse $CD8^+$ T cell isolation kit (Miltenyi Biotec). Total RNA was extracted from $CD8^+$ T cells with RNeasy Mini Kit (Qiagen) according to the manufacturer's instructions. Next-generation sequencing was performed with an unbiased TCR repertoire analysis technology (Repertoire Genesis Inc.) as described previously (16).

The detailed information for animal models, an ethics statement, histologic analysis, cytokine analysis, flow cytometric analysis, NK cell and $CD8^+$ cell depletion in vivo, safety assessment, and statistical analyses are described in the *SI Appendix, Supplementary Text*.

ACKNOWLEDGMENTS. We thank Kimberly Mcintyre, of the histology and imaging core, for the histological analysis and Howard B. Cottam and Angela Robles for editing the manuscript. This work was supported by the Immunotherapy Foundation (D.A.C.), Adjuvant Discovery Program (contracts HHSN272200900034C and HHSN272201400051C) (D.A.C.), and Japan Research Foundation for Clinical Pharmacology (T. Hosoya).

1. Steeg PS (2016) Targeting metastasis. *Nat Rev Cancer* 16:201–218.
2. Lambert AW, Pattabiraman DR, Weinberg RA (2017) Emerging biological principles of metastasis. *Cell* 168:670–691.
3. Mohammed T-LH, et al.; Expert Panel on Thoracic Imaging (2011) ACR Appropriateness Criteria® screening for pulmonary metastases. *J Thorac Imaging* 26:W1–W3.
4. Kitamura T, Qian BZ, Pollard JW (2015) Immune cell promotion of metastasis. *Nat Rev Immunol* 15:73–86.
5. Ostrand-Rosenberg S, Fenselau C (2018) Myeloid-derived suppressor cells: Immune-suppressive cells that impair antitumor immunity and are sculpted by their environment. *J Immunol* 200:422–431.
6. Sharma P, Allison JP (2015) Immune checkpoint targeting in cancer therapy: Toward combination strategies with curative potential. *Cell* 161:205–214.
7. Wolchok JD, et al. (2013) Nivolumab plus ipilimumab in advanced melanoma. *N Engl J Med* 369:122–133.
8. Brahmer J, et al. (2015) Nivolumab versus docetaxel in advanced squamous-cell non-small-cell lung cancer. *N Engl J Med* 373:123–135.
9. Wolchok JD, et al. (2017) Overall survival with combined nivolumab and ipilimumab in advanced melanoma. *N Engl J Med* 377:1345–1356.
10. Geisse J, et al. (2004) Imiquimod 5% cream for the treatment of superficial basal cell carcinoma: Results from two phase III, randomized, vehicle-controlled studies. *J Am Acad Dermatol* 50:722–733.
11. Savage P, et al. (1996) A phase I clinical trial of imiquimod, an oral interferon inducer, administered daily. *Br J Cancer* 74:1482–1486.
12. Engel AL, Holt GE, Lu H (2011) The pharmacokinetics of toll-like receptor agonists and the impact on the immune system. *Expert Rev Clin Pharmacol* 4:275–289.

13. Chan M, et al. (2009) Synthesis and immunological characterization of toll-like receptor 7 agonistic conjugates. *Bioconjug Chem* 20:1194–1200.
14. Wu CCN, et al. (2014) Innate immune protection against infectious diseases by pulmonary administration of a phospholipid-conjugated TLR7 ligand. *J Innate Immun* 6: 315–324.
15. Hayashi T, et al. (2011) Additive melanoma suppression with intralesional phospholipid-conjugated TLR7 agonists and systemic IL-2. *Melanoma Res* 21:66–75.
16. Sato-Kaneko F, et al. (2017) Combination immunotherapy with TLR agonists and checkpoint inhibitors suppresses head and neck cancer. *JCI Insight* 2:93397.
17. Wang D, et al. (2010) Antitumor activity and immune response induction of a dual agonist of toll-like receptors 7 and 8. *Mol Cancer Ther* 9:1788–1797.
18. Koga-Yamakawa E, et al. (2013) Intratracheal and oral administration of SM-276001: A selective TLR7 agonist, leads to antitumor efficacy in primary and metastatic models of cancer. *Int J Cancer* 132:580–590.
19. Cherfils-Vicini J, et al. (2010) Triggering of TLR7 and TLR8 expressed by human lung cancer cells induces cell survival and chemoresistance. *J Clin Invest* 120:1285–1297.
20. Chatterjee S, et al. (2014) TLR7 promotes tumor progression, chemotherapy resistance, and poor clinical outcomes in non-small cell lung cancer. *Cancer Res* 74:5008–5018.
21. Ochi A, et al. (2012) Toll-like receptor 7 regulates pancreatic carcinogenesis in mice and humans. *J Clin Invest* 122:4118–4129.
22. Dajon M, Iribarren K, Cremer I (2015) Dual roles of TLR7 in the lung cancer microenvironment. *Oncoimmunology* 4:e991615.
23. Pulaski BA, Ostrand-Rosenberg S (2001) Mouse 4T1 breast tumor model. *Curr Protoc Immunol* Chapter 20:Unit 20.2.
24. Ikeda Y, et al. (2017) Clinical significance of T cell clonality and expression levels of immune-related genes in endometrial cancer. *Oncol Rep* 37:2603–2610.
25. Subudhi SK, et al. (2016) Clonal expansion of CD8 T cells in the systemic circulation precedes development of ipilimumab-induced toxicities. *Proc Natl Acad Sci USA* 113: 11919–11924.
26. Straten PT, et al. (1998) Activation of preexisting T cell clones by targeted interleukin 2 therapy. *Proc Natl Acad Sci USA* 95:8785–8790.
27. Kim JA, et al. (2004) CDR3 spectratyping identifies clonal expansion within T-cell subpopulations that demonstrate therapeutic antitumor activity. *Surgery* 136:295–302.
28. Fernandez-Poma SM, et al. (2017) Expansion of tumor-infiltrating CD8+T cells expressing PD-1 improves the efficacy of adoptive T-cell therapy. *Cancer Res* 77: 3672–3684.
29. Yoshida R, et al. (2000) A new method for quantitative analysis of the mouse T-cell receptor V region repertoires: Comparison of repertoires among strains. *Immunogenetics* 52:35–45.
30. Zhang L, et al. (2017) 3D: Diversity, dynamics, differential testing - a proposed pipeline for analysis of next-generation sequencing T cell repertoire data. *BMC Bioinformatics* 18:129.
31. Goff PH, et al. (2015) Synthetic toll-like receptor 4 (TLR4) and TLR7 ligands as influenza virus vaccine adjuvants induce rapid, sustained, and broadly protective responses. *J Virol* 89:3221–3235.
32. Godebu E, et al. (2014) PCSD1, a new patient-derived model of bone metastatic prostate cancer, is castrate-resistant in the bone-niche. *J Transl Med* 12:275.
33. Liu C, et al. (2007) Expansion of spleen myeloid suppressor cells represses NK cell cytotoxicity in tumor-bearing host. *Blood* 109:4336–4342.
34. Hart OM, Athie-Morales V, O'Connor GM, Gardiner CM (2005) TLR7/8-mediated activation of human NK cells results in accessory cell-dependent IFN-gamma production. *J Immunol* 175:1636–1642.
35. Kasai M, Iwamori M, Nagai Y, Okumura K, Tada T (1980) A glycolipid on the surface of mouse natural killer cells. *Eur J Immunol* 10:175–180.
36. Hayashi T, et al. (2008) Mast cell-dependent anorexia and hypothermia induced by mucosal activation of toll-like receptor 7. *Am J Physiol Regul Integr Comp Physiol* 295: R123–R132.
37. Perkins H, et al. (2012) Therapy with TLR7 agonists induces lymphopenia: Correlating pharmacology to mechanism in a mouse model. *J Clin Immunol* 32:1082–1092.
38. Valastyan S, Weinberg RA (2011) Tumor metastasis: Molecular insights and evolving paradigms. *Cell* 147:275–292.
39. Topalian SL, Taube JM, Anders RA, Pardoll DM (2016) Mechanism-driven biomarkers to guide immune checkpoint blockade in cancer therapy. *Nat Rev Cancer* 16:275–287.
40. Spitzer MH, et al. (2017) Systemic immunity is required for effective cancer immunotherapy. *Cell* 168:487–502.e15.
41. Venturi V, Price DA, Douek DC, Davenport MP (2008) The molecular basis for public T-cell responses? *Nat Rev Immunol* 8:231–238.
42. Trautmann L, et al. (2005) Selection of T cell clones expressing high-affinity public TCRs within human cytomegalovirus-specific CD8 T cell responses. *J Immunol* 175: 6123–6132.
43. Miyama T, et al. (2017) Highly functional T-cell receptor repertoires are abundant in stem memory T cells and highly shared among individuals. *Sci Rep* 7:3663.
44. Cho HJ, et al. (2002) IFN-alpha beta promote priming of antigen-specific CD8+ and CD4+ T lymphocytes by immunostimulatory DNA-based vaccines. *J Immunol* 168: 4907–4913.
45. Hagemann T, et al. (2005) Macrophages induce invasiveness of epithelial cancer cells via NF-kappa B and JNK. *J Immunol* 175:1197–1205.
46. Sanmarco LM, et al. (2017) IL-6 promotes M2 macrophage polarization by modulating purinergic signaling and regulates the lethal release of nitric oxide during Trypanosoma cruzi infection. *Biochim Biophys Acta* 1863:857–869.
47. Quail DF, Joyce JA (2013) Microenvironmental regulation of tumor progression and metastasis. *Nat Med* 19:1423–1437.
48. Smits ELJM, Ponsaerts P, Berneman ZN, Van Tendeloo VFI (2008) The use of TLR7 and TLR8 ligands for the enhancement of cancer immunotherapy. *Oncologist* 13:859–875.
49. National Research Council (2011) *Guide for the Care and Use of Laboratory Animals* (National Academies Press, Washington, DC), 8th Ed.